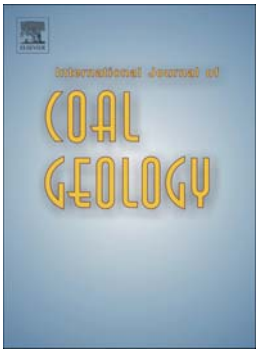


# Synergy of CuO and $CeO_2$ combination for mercury oxidation under low-temperature selective catalytic reduction atmosphere

Hailong Li, Lei Zhu, Shaokang Wu, Yang Liu, Kaimin Shih

PII: S0166-5162(16)30381-0
DOI: doi: 10.1016/j.coal.2016.07.011
Reference: COGEL 2682

To appear in: *International Journal of Coal Geology*

Received date: 22 January 2016
Revised date: 15 May 2016
Accepted date: 16 July 2016

Please cite this article as: Li, Hailong, Zhu, Lei, Wu, Shaokang, Liu, Yang, Shih, Kaimin, Synergy of CuO and $CeO_2$ combination for mercury oxidation under low-temperature selective catalytic reduction atmosphere, *International Journal of Coal Geology* (2016), doi: 10.1016/j.coal.2016.07.011

# Synergy of CuO and $CeO_2$ combination for mercury oxidation under low-temperature selective catalytic reduction atmosphere

*Hailong Li[1,3], Lei Zhu[1], Shaokang Wu[1], Yang Liu[2], Kaimin Shih[3*]*

1 School of Energy Science and Engineering, Central South University, Changsha, 410083, China

2 Advanced Membrane and Porous Materials Center, King Abdullah University of Science and Technology, Thuwal, 23955-6900, Kingdom of Saudi Arabia

3 Department of Civil Engineering, The University of Hong Kong, Hong Kong SAR, China

Revision submitted to **International Journal of Coal Geology**

*To whom correspondence should be addressed:

TEL: 852-28591973

FAX: 852-25595337

Email: kshih@hku.hk

**ABSTRACT:** Synergy for low temperature $Hg^0$ oxidation under selective catalytic reduction (SCR) atmosphere was achieved when copper oxides and cerium oxides were combined in a $CuO\text{-}CeO_2/TiO_2$ (CuCeTi) catalyst. $Hg^0$ oxidation efficiency as high as 99.0% was observed on the CuCeTi catalyst at 200 °C, even the gas hourly space velocity was extremely high. To analyze the synergistic effect, comparisons of catalyst performance in the presence of different SCR reaction gases were systematically conducted over $CuO/TiO_2$ (CuTi), $CeO_2/TiO_2$ (CeTi) and CuCeTi catalysts prepared by sol-gel method. The interactions between copper oxides and cerium oxides in CuCeTi catalyst yielded more surface chemisorbed oxygen, and facilitated the conversion of gas-phase $O_2$ to surface oxygen, which are favorable for $Hg^0$ oxidation. Copper oxides in the combination interacted with NO forming more chemisorbed oxygen for $Hg^0$ oxidation in the absence of gas-phase $O_2$. Cerium oxides in the combination promoted $Hg^0$ oxidation through enhancing the transformations of NO to $NO_2$. In the absence of NO, $NH_3$ exhibited no inhibitive effect on $Hg^0$ oxidation, because enough Lewis acid sites due to the combination of copper oxides and cerium oxides scavenged the competitive adsorption between $NH_3$ and $Hg^0$. In the presence of NO, although $NH_3$ lowered $Hg^0$ oxidation rate through inducing reduction of oxidized mercury, complete recovery of $Hg^0$ oxidation activity over the CuCeTi catalyst was quickly achieved after cutting off $NH_3$. This study revealed the synergistic effect of the combination of copper oxides and cerium oxides on $Hg^0$ oxidation, and explored the involved mechanisms. Such knowledge would help obtaining maximum $Hg^0$ oxidation co-benefit from SCR units in coal-fired power plants.

**KEYWORDS:** Mercury oxidation; Copper oxide; Cerium oxide; Selective catalytic reduction

## Introduction

Concerns about mercury pollution have been increasing since the notorious Minamata disease occurred in Japan in 1950s. According to the Global mercury assessment report 2013 ( United Nations Environment Programme, 2014), most of the anthropogenic mercury emission to air is from coal combustion, most notably in utility boilers. Because of the extreme toxicity, persistence, and bioaccumulation of methyl mercury transformed from emitted mercury (Pavlish et al., 2003), China and the United States (U.S.) already adopted national/federal mercury standards to limit mercury emission from coal-fired power plants by December 2011 (United States Environmental Protection Agency, 2011; Ministry of Environmental Protection of the People's Republic of China, 2011). Moreover, the Minamata Convention on Mercury, which is a global treaty to protect human health and the environment from the adverse effects of mercury, was agreed at the fifth session of the Intergovernmental Negotiating Committee in Geneva, Switzerland, on 19 January 2013. With the global and regional regulations on Mercury taking effect, technologies with higher efficiency and lower cost are urgently needed for controlling mercury emissions from coal-fired power plants.

Mercury in coal combustion flue gas presents in three forms, i.e. elemental mercury ($Hg^0$), oxidized mercury ($Hg^{2+}$), and particulate bound mercury ($Hg_p$) (Zhuang et al., 2004; Li et al., 2013). Among these mercury species, $Hg^0$ vapor is most likely to escape from existing air pollution control devices because it is highly volatile and nearly insoluble in water (Galbreath and Zygarlicke, 1996). Unfortunately, $Hg^0$ is the dominant mercury species emitted to the atmosphere, i.e. $Hg^0$ accounts for 66-94% of total mercury emitted from coal-fired power plants in China (Wang et al., 2010), and 67% for coal-fired power plants in Texas (Galbreath et al., 2005). In contrast, $Hg^{2+}$ can be easily absorbed by wet flue gas desulfurization (WFGD) solutions, since it is less volatile and water-soluble. Therefore,

maximizing the amount of $Hg^{2+}$ in the flue gas upstream of a WFGD system would offer a low-cost option for the control of mercury emission from coal-fired power plants (Senior, 2006).

Metal oxide based selective catalytic reduction (SCR) catalysts, originally employed to remove nitrogen oxides ($NO_x$) from flue gas, happen to be able to facilitate the oxidation of $Hg^0$ to $Hg^{2+}$ (Presto and Granite, 2006). As such, SCR system combining with WFGD would be promising for mercury removal from coal combustion flue gas (Reddy et al., 2012). The efficiency of this method depends largely on the conversion of $Hg^0$ to $Hg^{2+}$ over SCR catalysts (Pritchard, 2009). Therefore, studies about $Hg^0$ oxidation have been conducted over a variety of SCR catalysts (Richardson et al., 2002; Eswaran and Stenger, 2005; Senior, 2006, Cao et al., 2007; Pudasainee et al., 2010; Liu et al., 2011; Liu et al., 2011; Gao et al., 2013). Among these SCR catalysts, vanadia ($V_2O_5$) based commercial SCR catalysts have been demonstrated to be highly active for $Hg^0$ conversion (Gao et al., 2013). However, high operating temperature requirement for $V_2O_5$ based commercial SCR catalysts demands the SCR unit to be located upstream of a particulate matter control devices (PMCDs), where deactivation of these catalysts due to exposure to high concentration of particulate matter is severe. Ideally SCR catalysts should be active at low temperatures, which warrant them to be placed downstream of the PMCDs where flue gas is much cleaner (Li et al., 2012).

Ceria ($CeO_2$) based catalysts have been demonstrated to be efficient for low-temperature selective catalytic reduction of $NO_x$ by ammonia ($NH_3$) (Xu et al., 2008; Gao et al., 2010; Gao et al., 2010), due to the facile $Ce^{4+}/Ce^{3+}$ redox cycle which leads to higher oxygen storage capacity with reversible addition and removal of oxygen in the fluorite structure of ceria. In our previous study, a $CeO_2$ based catalyst has also been demonstrated to be able to facilitate $Hg^0$ oxidation even under low-rank coal combustion flue gas conditions (Li et al., 2011). Although $CeO_2$ based catalysts exhibit excellent

performance in catalytic processes, incorporation of other metal oxides into the $CeO_2$ lattice is generally agreed to obtain better redox properties than those of $CeO_2$ alone (Shan et al., 2003). For example, copper and cerium binary oxides ($CuO$-$CeO_2$) catalysts exhibited excellent catalytic activities toward NO reduction (Guo et al., 2014). Cyclic voltammetry investigations and temperature-programmed reaction studies confirmed that interactions between CuO and $CeO_2$ played important roles in enhancing the catalytic activity (Bera et al., 2001; Shan et al., 2003). Besides, pristine $CeO_2$ doesn't perform well in real catalysis due to the poor thermal stability (Zhang et al., 2012). Incorporation of copper into fluorite-type crystal structure of ceria was reported to improve the thermal stability of ceria based catalyst and enhance the oxygen storage capacities simultaneously (Wang et al., 2005). Moreover, $CeO_2$ based catalysts are sensitive to sulfur poisoning, because the highly active oxygen species of $CeO_2$ is also a strong oxidizer for sulfur dioxide ($SO_2$) (Casapu et al., 2009; Xu et al., 2009). By incorporating CuO into the formula, the $CuO$-$CeO_2$ mixed oxides exhibited excellent $SO_2$ resistance in selective catalytic reduction of NO with $NH_3$ (Du et al., 2012). As expected, $CuO$-$CeO_2$ binary oxides supported on titania ($TiO_2$) exhibited superior catalytic activity for low temperature $NO_x$ reduction by $NH_3$ (Gao et al., 2010; Li et al., 2015; Wu et al., 2015). In contrast, limited literatures reported the synergistic effect of the combination of copper oxides and cerium oxides (abbreviated in this paper as CuO and $CeO_2$ combination) in SCR catalyst for $Hg^0$ oxidation and even less the mechanisms responsible for the synergistic effect. To obtain the co-benefit of low temperature SCR catalysts containing copper oxides and cerium oxides for $Hg^0$ oxidation, a study on the synergistic effect of CuO and $CeO_2$ combination for $Hg^0$ oxidation under low temperature SCR atmosphere is urgently needed.

In this study, $Hg^0$ oxidation over $CuO$-$CeO_2$/$TiO_2$ (CuCeTi) catalyst prepared by a sol-gel method was studied under low temperature SCR atmosphere. The focus was obtaining and analyzing the

synergistic effect for $Hg^0$ oxidation when copper oxides and cerium oxides were combined together. Comparisons of catalyst performances in the presence of different SCR reaction gases were systematically conducted over $CuO/TiO_2$ (CuTi), $CeO_2/TiO_2$ (CeTi) and CuCeTi catalysts. The improved understanding of the synergistic effect of CuO and $CeO_2$ combination on $Hg^0$ oxidation would help optimizing catalyst design to obtain maximum co-benefit from SCR unit for removing $Hg^0$ from coal combustion flue gas.

**Experimental Section**

**Preparation and Characterization of Catalysts.** The CuTi, CeTi, and CuCeTi catalysts were synthesized by a sol-gel method which has been reported in our previous study (Li et al., 2015). In detail, aqueous solution of butyl titanate (99.5 wt%, Aladdin) and anhydrous ethanol (analytical grade, Sinopharm) was dropwise (less than 0.5 mL $min^{-1}$) added to another solution consisting of deionized water, anhydrous ethanol, nitric acid (analytical grade, Sinopharm), stoichiometric amounts of cerium nitrate (hexahydrate, 99.95 wt%, Aladdin) and/or copper nitrate (trihydrate, 99.5 wt%, Aladdin). The procedure was carried at room temperature under vigorous stirring to produce hydrolysis. After 3 h continuous stirring, the mixture was dried at 80 °C for 24 h, then calcined at 500 °C in the air for 4 h. Powder form catalysts were extracted by grinding the mixed-oxides and sieving through 80 meshes. The mass ratio of $(CuO+CeO_2)/TiO_2$ for the CuCeTi catalyst fixed at 0.6. The molar ratio of $CuO/CeO_2$ for the CuCeTi was 0.2. For comparison, the mass ratio of $CeO_2/TiO_2$ for the CeTi catalyst was 0.6, and CuO content in the CuTi catalyst was the same as that in the CuCeTi catalyst.

Brunauer-Emmett-Teller (BET) surface area measurement by $N_2$ adsorption/desorption at -196 °C was performed on an ASAP-2020 (Micromeritics, USA) BET analyzer. Before the BET analysis, each sample was oven dried at 110 °C for 24 h, and degassed at 180 °C for another 12 h under vacuum

condition. Powder X-ray diffraction (XRD) measurements were carried out on an X'Pert PRO diffractometer (PANalytical, Holland) with Cu Kα radiation (λ=0.15406 nm). The tube voltage and current were 40 kV and 40 mA, respectively. X-ray photoelectron spectroscopy (XPS) spectra was recorded using an Escalab 250Xi (Thermo Fisher Scientific, USA), and Al Kα monochromate (hv=1486.6 eV) was used as the excitation source. All oven-dried samples were degassed in a vacuum oven for at least 12 h prior to the XPS analysis. The vacuum of the XPS equipment was maintained at $10^{-6}$ Pa. Sample charging effects were eliminated by correcting the observed spectra with the C 1s binding energy (BE) value of 284.6 eV. Temperature programmed reduction experiments with hydrogen ($H_2$-TPR) were conducted in a U-shaped tubular quartz reactor to study the reducibility of catalysts. Prior to the $H_2$-TPR experiments, 0.10 g samples were pretreated at 300 °C in helium for 1 h. The samples were then cooled down to 50 °C in helium stream. Afterwards, the temperature of samples increased from 50 to 950 °C at a heating rate of 10 °C·min$^{-1}$ under $H_2$ (5 vol. %) /He flow with a total flow rate of 50 mL·min$^{-1}$. $H_2$ consumption during the experiments was monitored continuously by a PX200 thermal conductivity detector.

**Fixed-bed Experiments.** The evaluation of $Hg^0$ oxidation performances was conducted on a bench-scale fixed-bed system shown in Figure 1. In each test, 0.20 to 0.80 g different catalysts were loaded into a borosilicate glass reactor with inner diameter of 10 mm. The glass reactor was placed in a temperature controlled tubular furnace to maintain the reaction temperature to be 200 °C. Cylinder gases were used to provide individual flue gas components, i.e., $N_2$, $O_2$, NO, and $NH_3$. The gas flow rates were precisely controlled by mass flow controllers, and the total flow rate kept at 1000 mL·min$^{-1}$. A constant $Hg^0$ feed (75 μg·m$^{-3}$) was provided by a Dynacal $Hg^0$ permeation device (VICI Metronics). The relatively high $Hg^0$ concentration was employed to reduce experimental errors caused by the sensitivity

of the mercury analyzer and to allow experiments to be completed in a reasonable time scale. $Hg^0$ concentrations at both the inlet and outlet of the reactor were online monitored by a VM3000 mercury analyzer (Mercury Instruments Inc., Germany). To avoid the adverse effect of water vapor on $Hg^0$ measurement and any possible damage to the instrument, trace amount of water vapor in the gas flow was removed by silica before entering into the mercury analyzer. The exhaust gas was treated by chlorinate activated carbon before discharge.

Firstly, 0.80 g of CuTi, CeTi and CuCeTi catalysts were used to investigate the synergistic effect of CuO and $CeO_2$ combination on $Hg^0$ oxidation under low temperature SCR atmosphere, which was defined in this study as 1000 ppm NO, 1000 ppm $NH_3$, and 4% $O_2$ balanced in $N_2$ at 200 °C. For each catalyst, triplicate experiments were conducted, and their mean values and standard deviations were reported. To explore the involved mechanisms, $Hg^0$ oxidation over 0.20 g of different catalysts was systematically studied in the presence of different gas components. CuCeTi catalyst with different dosages (0.20-0.80 g) was also adopted to study the effect of $NH_3$ on $Hg^0$ oxidation in the presence of NO. Before these experiments, an empty bed experiment was conducted, and the results of which demonstrated the interferences on $Hg^0$ measurement by an empty reactor and gas components within the concentration range studied were negligible.

At the beginning of each test, the gas stream bypassed the reactor and the inlet gas was monitored until the desired inlet $Hg^0$ concentration ($[Hg^0]_{inlet}$) had been stabilized for at least 30 min. The gas flow was then passed through the reactor, and taken from the exit of the reactor to measure the outlet $Hg^0$ concentration ($[Hg^0]_{outlet}$). For calculating the $Hg^0$ oxidation efficiency ($E_{oxi}$), $[Hg^0]_{outlet}$ was recorded after the catalytic process had reached equilibrium, which was defined as having fluctuations of $Hg^0$

concentration less than 5% for more than 30 min. At the end of each experiment, the inlet gas was sampled again to verify the $[Hg^0]_{inlet}$. $E_{oxi}$ in this study was calculated by equation (1).

$$E_{oxi} = ([Hg^0]_{inlet} - [Hg^0]_{outlet})/[Hg^0]_{inlet} \times 100\% \quad (1)$$

**Results and Discussions**

**Characterization of catalysts.** Among the three different catalysts, CuTi exhibited the lowest surface area of 66.8 $m^2 \cdot g^{-1}$. CeTi showed the highest surface areas of 101.4 $m^2 \cdot g^{-1}$, which is much higher than that of a CeTi catalyst prepared by wet impregnation method (Li et al., 2011). The addition of copper oxides slightly lowered the surface area of CeTi catalyst, and the surface area of CuCeTi was 95.0 $m^2 \cdot g^{-1}$.

The XRD patterns of CuTi, CeTi and CuCeTi catalysts have been presented in our previous study (Li, et al., 2015). No CuO characteristic peak on the XRD patterns of CuTi and CuCeTi catalysts suggests that copper species were well dispersed on the $TiO_2$ support and/or incorporated into the lattice of $CeO_2$ (Avgouropoulos and Ioannides, 2006). For CeTi and CuCeTi catalysts, characteristic peaks corresponding to cubic $CeO_2$ were observed to be weak and broad, indicating that $CeO_2$ was well dispersed. $Ti^{4+}$ could probably incorporate into the $CeO_2$ lattice (Luo et al., 2000), and hence lowered $TiO_2$ peak intensity for the CeTi and CuCeTi catalysts. Compare to the XRD pattern of CeTi catalyst, $CeO_2$ peaks on the XRD pattern of CuCeTi catalyst became weaker, indicating there were interactions between copper oxides and cerium oxides. One possible interaction was that $Cu^{2+}$ ions incorporated into ceria lattice, as the radius of $Cu^{2+}$ ion (0.072 nm) is smaller than that of $Ce^{4+}$ ion (0.101 nm) (Shan et al., 2003). The defective structure of $CeO_2$ lattice could promote the formation of more chemisorbed oxygen on the catalyst surface (Guo et al., 2014), which is the most active oxygen and plays an

important role in oxidation reactions such as $Hg^0$ oxidation (Li et al., 2011) and $NH_3$ activation (Qi and Yang, 2004).

The XPS spectra of Cu 2p for CuTi and CuCeTi catalysts are displayed in Figure 2(a). As shown, both catalysts exhibited a peak of Cu $2p_{3/2}$ at 934.3 eV, a peak of Cu $2p_{1/2}$ at 953.7 eV, and a shake-up peak located in the binding energy range of 938-945 eV, which are the characteristics of $Cu^{2+}$ species (Liu et al., 2011; Chen et al., 2013; Yao et al., 2014). Characteristic peaks at 932.2 eV for Cu $2p_{3/2}$ and peaks at 952.0 eV for Cu $2p_{1/2}$ were ascribed to the existence of $Cu^+$ species on the CuTi and CuCeTi catalysts (Si et al., 2010; Si et al., 2011). The appearance of $Cu^+$ species was probably owing to the redox cycles of $Cu^{2+} + Ti^{3+} \leftrightarrow Cu^+ + Ti^{4+}$, and $Cu^{2+} + Ce^{3+} \leftrightarrow Cu^+ + Ce^{4+}$ shifting to right (Yao et al., 2013; Yao et al., 2014). The percent content of $Cu^+$ can be determined by calculating the corresponding peak areas, and lists in Table 1. In comparison with the CuTi catalyst, more $Cu^{2+}$ were reduced to $Cu^+$ on the surface of the CuCeTi catalyst, indicating there were interactions between cerium oxides and copper oxides when they combined together.

The XPS spectra of Ce 3d for CeTi and CuCeTi catalysts are shown in Figure 2(b). The curves of Ce 3d spectra consisted of eight peaks referring to four pairs of spin-orbit doublets. The sub-bands labeled v, v2, v3, u, u2, and u3 referred to the $3d^{10}4f^0$ initial electronic state of $Ce^{4+}$ while the other two bands labeled v1 and u1 were ascribed to the $3d^{10}4f^1$ initial electronic state of $Ce^{3+}$ (Li et al., 2011; Wang et al., 2012). For both catalysts, peaks attributed to $Ce^{4+}$ were predominant, while the small peaks of v1 evidenced the presence of $Ce^{3+}$ over the CeTi and CuCeTi catalysts. As shown in Table 1, the combination of copper oxides and cerium oxides resulted in more $Ce^{3+}$ on the CuCeTi catalyst. The presence of $Ce^{3+}$ could create charge imbalance, oxygen vacancies and unsaturated chemical bonds on the catalyst surface (Yang et al., 2006). Therefore, the combination of copper oxides and cerium oxides

yielded more chemisorbed oxygen species (shown in Table 1) on the CuCeTi catalyst, which are highly active in redox processes (Chen et al., 2009).

The $H_2$-TPR profiles of the three different catalysts also have been reported (Li et al., 2015). It should be noted that the first reduction peak for CuTi, CeTi, and CuCeTi were at 180, 503, and 160 °C, respectively (as shown in Table 1). The combination of copper oxides and cerium oxides resulted in lower reduction temperature, which warrants CuCeTi catalyst to be more active than CuTi and CeTi catalysts for low temperature $Hg^0$ oxidation.

**Synergistic effect of the CuO and $CeO_2$ combination on $Hg^0$ oxidation.** $Hg^0$ oxidation efficiencies over CuTi, CeTi and CuCeTi catalysts under SCR atmosphere at 200 °C are shown in Figure 3. As shown, $E_{oxi}$ over the CuTi catalyst was about 90.0%. This indicates that CuTi catalyst is active for $Hg^0$ oxidation under low-temperature SCR atmosphere with no hydrogen chloride (HCl) presence. $E_{oxi}$ over the CeTi catalyst was 52.7%, which is lower than that for CuTi catalyst. This is agreed with other research that CuTi catalyst is more active than CeTi catalyst for $Hg^0$ oxidation at low temperatures (Xu et al., 2014). $E_{oxi}$ for the CuCeTi catalyst was 99.0%, which is much higher than that for CuTi and CeTi catalysts. This result demonstrates the existence of synergy in $Hg^0$ oxidation when copper oxides and cerium oxides were combined. This is similar to other research (Gao et al., 2010) where CuCeTi catalyst was reported to be more effective than CuTi and CeTi catalyst for selective catalytic reduction of $NO_x$ by $NH_3$. This is also in accordance with the XRD and XPS results that the interactions between copper oxides and cerium oxides resulted in more active chemisorbed oxygen, which could facilitate $Hg^0$ oxidation. Moreover, the superior low-temperature activity of CuCeTi catalyst was also in line with the $H_2$-TPR results that CuCeTi catalyst is more active at low temperatures than CuTi and CeTi catalysts.

As most oxidized mercury species in real coal combustion flue gas exists as $HgCl_2$ (Cao et al., 2008), HCl is widely agreed to be the most important flue gas component responsible for $Hg^0$ oxidation. In this study, no HCl was added to the simulated flue gas to promote $Hg^0$ oxidation. The co-presence of NO and $NH_3$ would probably induce the reduction of oxidized mercury (Li et al., 2015), which lowers the observed $Hg^0$ oxidation efficiency. Moreover, the gas hourly space velocity (GHSV) of 54, 000 $h^{-1}$ corresponding to 0.80 g catalyst was much higher than the typical GHSV (2000-4000 $h^{-1}$) in power plant SCR reactors (Laudal, 2002). Even though the contacting conditions in fix-bed is better than that of the actual SCR reactor, the results still imply that applications of the CuCeTi catalyst as a low temperature SCR catalyst very likely are beneficial to $Hg^0$ oxidation in coal-fired power plants, because more HCl, less $NH_3$, and lower space velocity can facilitate $Hg^0$ conversion. Furthermore, an even better catalytic performance could probably be obtained by optimizing the CuCeTi constitute such as the ratio of CuO and $CeO_2$ in future studies.

**Understanding the synergistic effect by comparison of catalyst performances under different gas atmospheres.** As a promising low-temperature SCR catalyst, CuCeTi catalyst is originally designed for facilitating $NO_x$ reduction by $NH_3$ (Gao et al., 2010). Similar to $NO_x$ selective catalytic reduction process, synergy for $Hg^0$ oxidation in the presence of $N_2$, $O_2$, NO, and $NH_3$ was achieved when copper oxides and cerium oxides were combined. To explore the mechanisms responsible for the synergistic effect on $Hg^0$ oxidation, comparison of $Hg^0$ oxidation performance at 200 °C were conducted over the CuTi, CeTi, and CuCeTi catalysts in the presence of individual flue gas components, i.e., $N_2$, $O_2$, NO, and $NH_3$.

**$Hg^0$ oxidation in pure $N_2$ atmosphere.** $Hg^0$ oxidation over different catalysts in the presence of $N_2$ alone is shown in Figure 4. As shown, gas flow containing $N_2$ and 75 $\mu g \cdot m^{-3}$ $Hg^0$ passed through 0.20 g

catalysts from point "a" (about 0.5 h) to point "b" (about 2.5 h). After passing through CuTi catalyst, normalized outlet $Hg^0$ concentration (to inlet $Hg^0$ concentration) firstly dropped to about 0.6, and quickly climbed up to 0.8 in 2 hours, indicating that only a limited amount of $Hg^0$ adsorbed and/or oxidized on the CuTi catalyst at 200 °C in pure $N_2$ atmosphere. CeTi catalyst performed slightly better than CuTi catalyst under pure $N_2$ atmosphere. After switched gas flow to CeTi catalyst, normalized outlet $Hg^0$ concentration firstly dropped to about 0.4, and quickly climbed up to about 0.75 in 2 hours. In contrast, the normalized outlet $Hg^0$ concentration swiftly dropped to 0.2 after passing through the CuCeTi catalyst and remained around 0.2 during the entire 2 hours test. As shown in Figure 5, after passing through the CuCeTi catalyst at room temperature under pure $N_2$ atmosphere, $Hg^0$ concentration only dropped from 75 to about 50 $\mu g \cdot m^{-3}$, and suddenly rose up to 75 $\mu g \cdot m^{-3}$ in 10 minutes. This phenomenon demonstrates that $Hg^0$ physical adsorption capacity of the CuCeTi catalyst was negligible even through at room temperature. Therefore, the huge loss of $Hg^0$ on the CuCeTi catalyst under pure $N_2$ atmosphere was due to the reaction between $Hg^0$ and stored oxygen (Granite et al., 2000), especially the active chemisorbed oxygen (Li et al., 2012). CuO and $CeO_2$ combination in the CuCeTi catalyst yielded more surface chemisorbed oxygen, and hence resulted in more $Hg^0$ oxidation under pure $N_2$ atmosphere.

**$Hg^0$ oxidation with the aid of gas-phase $O_2$.** $Hg^0$ oxidation over different catalysts in the presence of 4% gas-phase $O_2$ is shown in Figure 6. As shown, the normalized outlet $Hg^0$ concentration swiftly dropped to about 0.5, 0.3, and 0.1, after passing through the CuTi, CeTi, and CuCeTi catalysts, respectively. For all catalysts, the normalized outlet $Hg^0$ concentration maintained almost constant during the entire 1.5 hours test. Comparing to the pure $N_2$ atmosphere, more $Hg^0$ oxidation was achieved over all catalysts with the aid of gas-phase $O_2$. This was due to that gas-phase $O_2$ continuously

regenerated the lattice oxygen and replenished the chemisorbed oxygen, which served as the $Hg^0$ oxidant (Li et al., 2011). In other word, $Hg^0$ should be oxidized to be HgO attached on the catalyst surface in the presence of gas-phase $O_2$. This phenomenon was identified by a XPS analysis of mercury saturated CuCeTi catalyst (Li et al., 2015). Similar to that under pure $N_2$ atmosphere, CuCeTi catalyst performed better than CuTi and CeTi catalysts in the presence of gas-phase $O_2$. This was not only ascribed to more surface chemisorbed oxygen on the CuCeTi catalyst surface but also probably due to the CuO and $CeO_2$ combination facilitated oxygen conversion between gas-phase $O_2$ and surface oxygen, which is efficient for $Hg^0$ oxidation.

**$Hg^0$ oxidation in the presence of NO.** Significant promotional effect of NO on $Hg^0$ oxidation was observed over the CuTi catalyst. As shown in Figure 4, a significant decrease of outlet $Hg^0$ concentration was observed downstream the CuTi catalyst after adding 500 ppm NO to the pure $N_2$ gas flow at point "b". Since $TiO_2$ is essentially inactive for the oxidation of $Hg^0$ (Kamata et al., 2008), $Hg^0$ oxidation observed was attributed to the activity of copper oxides supported on $TiO_2$. Without gas-phase $O_2$, NO interacted with reduced copper sites forming a dinitrosyl intermediate complex. The dinitrosyl intermediate complex subsequently decomposed to form $N_2$ or $N_2O$, and leaving active chemisorbed oxygen atoms (Centi and Perathoner, 1995), which are highly active for $Hg^0$ oxidation. In the absence of gas-phase $O_2$, NO slightly promoted $Hg^0$ oxidation over the CeTi catalyst at the first stage, then the promotional effect gradually receded, finally NO even exhibited inhibitive effect on $Hg^0$ oxidation. For the CuCeTi catalyst, NO also exhibited a negligible effect on $Hg^0$ oxidation in the absence of $O_2$. The outlet $Hg^0$ concentration in the presence of 500 ppm NO was just slightly lower than that under pure $N_2$ atmosphere. Further increase of NO concentration to 1000 ppm at point "c" did not change $Hg^0$ oxidation performance obviously. With the presence of NO, $Hg^0$ oxidation performances over the CuTi

and CuCeTi catalysts were close to each other, and much higher than that for the CeTi catalyst, indicating that copper oxides were more active than cerium oxides for $Hg^0$ oxidation under this $N_2$ plus NO atmosphere.

Negligible variation of $Hg^0$ oxidation over the CuTi catalyst was detected when 4% $O_2$ was added to gas flow containing 1000 ppm NO. In contrast, addition of 4% $O_2$ resulted in huge loss of $Hg^0$ downstream of the CeTi catalyst. This was mainly due to gas-phase $O_2$ continuously regenerated active surface oxygen which served as the $Hg^0$ oxidant, since the other gas component NO promoted $Hg^0$ oxidation over the CeTi catalyst negligibly (i.e., $E_{oxi}$ in the presence of 1000 ppm NO and 4% $O_2$ was slightly higher than that in the presence of 4% $O_2$ alone). This phenomenon demonstrates again that ceria based catalysts are good at converting gas-phase $O_2$ to surface oxygen. For the CuCeTi catalyst, an obvious promotional effect of NO on $Hg^0$ oxidation was observed in the presence of $O_2$. The outlet $Hg^0$ concentration in the co-presence of 1000 ppm NO and 4% $O_2$ (shown in Figure 4) was lower than that in the presence of 4% $O_2$ alone (shown in Figure 6). Cerium oxides in the CuCeTi catalyst facilitated the transformation of gas-phase $O_2$ to active surface oxygen, which gave rise to the formation of abundant active species like $NO_2$ on the catalyst surface (Li et al., 2008). These active species promoted $Hg^0$ oxidation.

In summary, copper oxides in the CuO and $CeO_2$ combination interacted with NO forming more chemisorbed oxygen for $Hg^0$ oxidation in the absence of gas-phase $O_2$. Meanwhile, cerium oxides in the CuO and $CeO_2$ combination enhanced the transformations of gas-phase $O_2$ to surface oxygen and NO to $NO_2$, which facilitate $Hg^0$ oxidation.

**$Hg^0$ oxidation with the presence of $NH_3$.** As shown in Figure 6, about 0.50 of feed $Hg^0$ was detected downstream the CuTi catalyst with the presence of 4% $O_2$. After adding 500 ppm $NH_3$, about 0.60 of

feed $Hg^0$ was detected downstream the catalyst. In the presence of gas-phase $O_2$, $NH_3$ slightly inhibited $Hg^0$ oxidation over the CuTi catalyst. In contrast, a huge increase of outlet $Hg^0$ concentration was observed after adding 500 ppm $NH_3$ to the CeTi system, indicating $NH_3$ greatly prohibited $Hg^0$ oxidation over the CeTi catalyst. $NH_3$ competes with $Hg^0$ for active sites on the CeTi catalyst (Li et al., 2015), and hence inhibited $Hg^0$ adsorption and subsequent oxidation.

$NH_3$ is known to primarily adsorb on Brønsted acid sites ( Topsøe, 1994; Madsen, 2011), while Lewis acid sites are more suitable for $Hg^0$ adsorption (Eom et al., 2008; Madsen, 2011). Generally, limited or no Brønsted acid sites are present on the CuO surface (Ramis et al., 1995; Kamata et al., 2009). In contrast, Brønsted acid sites and Lewis acid sites are present on the surface of ceria based catalysts (Xu et al., 2009; Chen et al., 2010). With a successive addition of CuO into a ceria based catalyst matrix, Brønsted acid sites were demonstrated to be stepwise substituted by Lewis acid sites (Yu et al., 2011). Therefore, it is reasonable to believe that the combination of CuO and $CeO_2$ in the CuCeTi catalyst yielded more Lewis acid sites for $Hg^0$ adsorption, and hence reduced the competitive adsorption between $NH_3$ and $Hg^0$, which has been confirmed by a desorption experiment in our previous study (Li et al., 2015). Moreover, the inhibitive effect of $NH_3$ on $Hg^0$ oxidation through consumption of surface oxygen can be completely scavenged in the presence of $O_2$ (Li et al., 2015). Therefore, addition of 500 ppm $NH_3$ to gas flow containing $O_2$ resulted in negligible effect on $Hg^0$ oxidation over the CuCeTi catalyst.

Due to the advantages of the CuO and $CeO_2$ combination, $NH_3$ alone exhibited no inhibitive effect on $Hg^0$ oxidation over the CuCeTi catalyst in the presence of $O_2$. However, a huge deactivation of $Hg^0$ oxidation over the CuCeTi catalyst was observed when NO was also present. As shown in Figure 7, the normalized outlet $Hg^0$ concentration downstream of 0.20 g CuCeTi catalyst rapidly rise from about 0.02

up to 0.36 when 1000 ppm $NH_3$ was introduced to a gas low containing 4% $O_2$ and 1000 ppm NO, and maintained around 0.40 during the entire 1.0 hour test. With the merits of the CuO and $CeO_2$ combination, neither NO nor $NH_3$ alone exhibited an inhibitive effect on $Hg^0$ oxidation in the presence of $O_2$. Because the observed oxidation rate of $Hg^0$ is the net sum of an oxidation and a reversed reduction reaction, the huge deactivation of $Hg^0$ oxidation over the CuCeTi catalyst in the co-presence of $O_2$, NO and $NH_3$ was probably due to reduction of oxidized mercury (Li et al., 2015), which usually took place in parallel with $Hg^0$ oxidation. With the increase of catalyst dosage from 0.20 g to 0.80 g, the normalized outlet $Hg^0$ concentration gradually decreased from about 0.40 to around 0.02, which is same as that without $NH_3$. When the catalyst layer became thicker, more $NH_3$-free or $NH_3$-deficient space at the tail-end of the catalyst layer was obtained, where the reduction of oxidized mercury was scavenged or at least relieved. Therefore, higher $Hg^0$ oxidation rate was observed. Even though $NH_3$ lowered $Hg^0$ oxidation rate in the presence of NO through inducing reduction of oxidized mercury, complete recovery of $Hg^0$ oxidation activity of the CuCeTi catalyst can be rapidly achieved after cutting off $NH_3$. As shown in Figure 7, the normalized outlet $Hg^0$ concentration quickly declined to about 0.02 when $NH_3$ was eliminated from the gas flow, regardless the catalyst dosage. With this merit of the CuCeTi catalyst, high $Hg^0$ oxidation efficiency can be easily achieved once $NH_3$ is consumed in the SCR reactions which primarily taking place in the front section of catalyst layer.

**Conclusion**

Obvious synergy in $Hg^0$ oxidation under SCR atmosphere was achieved when copper oxides and cerium oxides were combined in a low temperature CuCeTi catalyst. At 200 °C, $Hg^0$ oxidation efficiency as high as 99.0% was observed on the CuCeTi catalyst under SCR atmosphere with a GHSV more than 10 times higher than the actual GHSV in power plant SCR reactors. The interactions between

copper oxides and cerium oxides yielded more surface chemisorbed oxygen, which was responsible for $Hg^0$ oxidation under pure $N_2$ atmosphere. In the presence of gas-phase $O_2$, the CuO and $CeO_2$ combination facilitated oxygen conversion between gas-phase $O_2$ and surface oxygen, and hence facilitated $Hg^0$ oxidation. Copper oxides in the CuO and $CeO_2$ combination could interact with NO forming more chemisorbed oxygen for $Hg^0$ oxidation in the absence of gas-phase $O_2$. Cerium oxides in the CuO and $CeO_2$ combination could promote $Hg^0$ oxidation through enhancing the transformation of NO to $NO_2$. The CuO and $CeO_2$ combination resulted in enough Lewis acid sites for $Hg^0$ adsorption, and hence scavenged the competitive adsorption between $NH_3$ and $Hg^0$. Even though $NH_3$ lowered $Hg^0$ oxidation rate in the presence of NO, excellent $Hg^0$ oxidation activity can be obtained over the CuCeTi catalyst once there were $NH_3$-free or $NH_3$-deficient spaces at the tail-end of the catalyst layer. The synergistic effect of the CuO and $CeO_2$ combination on $Hg^0$ oxidation under SCR atmosphere warrants the CuCeTi catalyst to be a promising low-temperature SCR catalyst, on which co-benefit of $Hg^0$ emission control can be achieved.



**Acknowledgments**

This project was supported by the National Natural Science Foundation of China (NO. 51476189), the Hong Kong General Research Fund Scheme (No. 17206714), the Hong Kong Scholar Program (NO. XJ2014033), and the Key Research and Development Program of Hunan Province (No. 2015SK2007).

**References**

Avgouropoulos, G., Ioannides, T., 2006. Effect of synthesis parameters on catalytic properties of CuO-$CeO_2$. Applied Catalysis B-Environmental 67 (1-2), 1-11.

Bera, P., Mitra, S., Sampath, S., Hegde, M.S. 2001. Promoting effect of CeO in a Cu/CeO catalyst: lowering of redox potentials of Cu species in the CeO matrix. Chemical Communications 10, 927-928.

Cao, Y., Gao, Z., Zhu, J., Wang, Q., Huang, Y., Chiu, Chiu, C., Parker, B., Chu, P., Pan, W., 2007. Impacts of halogen additions on mercury oxidation, in a slipstream selective catalyst reduction (SCR), reactor when burning sub-bituminous coal. Environmental Science & Technology 42 (1), 256-261.

Casapu, M., Kröcher, O., Elsener, M., 2009. Screening of doped MnOx-$CeO_2$ catalysts for low-temperature NO-SCR. Applied Catalysis B: Environmental 88 (3-4), 413-419.

Centi, G., Perathoner, S., 1995. Nature of active species in copper-based catalysts and their chemistry of transformation of nitrogen oxides. Applied Catalysis A: General 132 (2), 179-259.

Chen, G.X., Li, Q.L., Wei, Y.C., Fang, W.P., Yang, Y.Q., 2013. Low temperature CO oxidation on Ni-promoted CuO-$CeO_2$ catalysts. Chinese Journal of Catalysis 34 (2), 322-329.

Chen, L., Li, J., Ge, M., 2009. Promotional effect of Ce-doped $V_2O_5$-$WO_3/TiO_2$ with low vanadium loadings for selective catalytic reduction of NOx by $NH_3$. Journal of Physical Chemistry C 113 (50), 21177-21184.

Chen, L., Li, J., Ge, M., 2010. DRIFT study on Cerium-Tungsten/Titiania catalyst for selective catalytic reduction of NOx with $NH_3$. Environmental Science & Technology 44 (24), 9590-9596.

Du, X.S., Gao, X., Cui, L.W., Fu, Y.C., Luo, Z.Y., Cen, K.F., 2012. Investigation of the effect of Cu addition on the $SO_2$-resistance of a CeTi oxide catalyst for selective catalytic reduction of NO with $NH_3$. Fuel 92 (1), 49-55.

Eom, Y., Jeon, S.H., Ngo, T.A., Kim, J., Lee, T.G., 2008. Heterogeneous mercury reaction on a selective catalytic reduction (SCR) catalyst. Catalysis Letters 121 (3-4), 219-225.

Eswaran, S., Stenger, H.G., 2005. Understanding mercury conversion in selective catalytic reduction (SCR) catalysts. Energy & Fuels 19 (6), 2328-2334.

Galbreath, K.C., Zygarlicke, C.J., 1996. Mercury speciation in coal combustion and gasification flue gases. Environmental Science & Technology 30 (8), 2421-2426.

Galbreath, K.C., Zygarlicke, C.J., Tibbetts, J.E., Schulz, R.L., Dunham, G.E., 2005. Effects of $NO_x$, alpha-$Fe_2O_3$, gamma-$Fe_2O_3$, and HCl on mercury transformations in a 7-kW coal combustion system. Fuel Processing Technology 86 (4), 429-448.

Gao, W., Liu, Q., Wu, C.Y., Li, H., Li, Y., Yang, J., Wu, G., 2013. Kinetics of mercury oxidation in the presence of hydrochloric acid and oxygen over a commercial SCR catalyst. Chemical Engineering Journal 220, 53-60.

Gao, X., Du, X.S., Cui, L.W., Fu, Y.C., Luo, Z.Y., Cen, K.F., 2010a. A Ce-Cu-Ti oxide catalyst for the selective catalytic reduction of NO with $NH_3$. Catalysis Communications 12 (4), 255-258.

Gao, X., Jiang, Y., Fu, Y., Zhong, Y., Luo, Z.Y., Cen, K.F., 2010b. Preparation and characterization of $CeO_2/TiO_2$ catalysts for selective catalytic reduction of NO with $NH_3$. Catalysis Communications 11 (5), 465-469.

Gao, X., Jiang, Y., Zhong, Y., Luo, Z.Y., Cen, K.F., 2010c. The activity and characterization of $CeO_2$-$TiO_2$ catalysts prepared by the sol-gel method for selective catalytic reduction of NO with $NH_3$. Journal of Hazardous Materials 174 (1-3), 734-739.

Gao, Y., Zhang, Z., Wu, J., Duan, L., Umar, A., Sun, L., Guo, Z., Wang, Q., 2013. A critical review on the heterogeneous catalytic oxidation of elemental mercury in flue gases. Environmental Science & Technology 47 (19), 10813-10823.

Guo, R.T., Zhen, W.L., Pan, W.G., Zhou, Y., Hong, J.N., Xu, H.J., Jin, Q., Ding, C.G., Guo, S.Y., 2014. Effect of Cu doping on the SCR activity of $CeO_2$ catalyst prepared by citric acid method. Journal of Industrial and Engineering Chemistry 20 (4), 1577-1580.

Granite, E. J., Pennline, H. W., Hargis, R. A., 2000. Novel Sorbents for Mercury Removal from Flue Gas. Industrial & Engineering Chemistry Research 39(4), 1020-1029.

Kamata, H., Ueno, S.I., Naito, T., Yamaguchi, A., Ito, S., 2008. Mercury oxidation by hydrochloric acid over a $VOx/TiO_2$ catalyst. Catalysis Communications 9 (14), 2441-2444.

Kamata, H., Ueno, S.I., Sato, N., Naito, T., 2009. Mercury oxidation by hydrochloric acid over $TiO_2$ supported metal oxide catalysts in coal combustion flue gas. Fuel Processing Technology 90 (7-8), 947-951.

Laudal, D.L., Thompson, J.S., Pavlish, J.H., Brickett, L., Chu, P., Srivastava, R.K., Lee, C.W., Kilgroe, J., 2002. Mercury speciation at power plants using SCR and SNCR control technologies. 3rd International Air Quality Conference, Arlington, Virginia.

Li, H., Wu, C.Y., Li, L., Li, Y., Zhao, Y., Zhang, J., 2013. Kinetic modeling of mercury oxidation by chlorine over $CeO_2$-$TiO_2$ catalysts. Fuel 113, 726-732.

Li, H., Wu, C.Y., Li, Y., Li, L., Zhao, Y., Zhang, J., 2012. Role of flue gas components in mercury oxidation over $TiO_2$ supported MnOx-$CeO_2$ mixed-oxide at low temperature. Journal of Hazardous Materials 243, 117-123.

Li, H., Wu, C.Y., Li, Y., Zhang, J., 2011. $CeO_2$-$TiO_2$ catalysts for catalytic oxidation of elemental mercury in low-rank coal combustion flue gas. Environmental Science & Technology 45 (17), 7394-7400.

Li, H., Wu, S., Li, L., Wang, J., Ma, W., Shih, K., 2015a. CuO-$CeO_2/TiO_2$ catalyst for simultaneous NO reduction and $Hg^0$ oxidation at low temperatures. Catalysis Science & Technology 5 (12), 5129-5138.

Li, H., Wu, S., Wu, C.Y., Wang, J., Li, L., Shih, K., 2015b. SCR atmosphere induced reduction of oxidized mercury over $CuO\text{-}CeO_2/TiO_2$ catalyst. Environmental Science & Technology 49 (12), 7373-7379.

Li, Y., Murphy, P.D., Wu, C.Y., Powers, K.W., Bonzongo, J.C.J., 2008. Development of Silica/Vanadia/Titania catalysts for removal of elemental mercury from coal-combustion flue gas. Environmental Science & Technology 42 (14), 5304-5309.

Liu, L., Yao, Z., Deng, Y., Gao, F., Liu, B., Dong, L., 2011. Morphology and crystal-plane effects of nanoscale ceria on the activity of $CuO/CeO_2$ for NO reduction by CO. Chemcatchem 3 (6), 978-989.

Liu, J., He, M., Zheng, C., Chang, M., 2011. Density functional theory study of mercury adsorption on $V_2O_5$ (001) surface with implications for oxidation. Proceedings of the Combustion Institute 33 (2), 2771-2777.

Luo, M., Chen, J., Chen, L., Lu, J., Feng, Z., Li, C., 2001. Structure and Redox Properties of $CexTi1\text{-}xO_2$ Solid Solution. Chemistry of Materials 13 (1), 197-202.

Madsen, K., 2011. Mercury Oxidation over Selective Catalytic Reduction (SCR) Catalysts. DTU Chemical Engineering, Department of Chemical and Biochemical Engineering.

Ministry of Environmental Protection of the People's Republic of China, 2011. Emission Standard of Air Pollutants for Thermal Power Plants, GB13223-2011. China Environmental Science Press, Beijing.

Pavlish, J.H., Sondreal, E.A., Mann, M.D., Olson, E.S., Galbreath, K.C., Laudal, D.L., Benson, S.A., 2003. Status review of mercury control options for coal-fired power plants. Fuel Processing Technology 82 (2), 89-165.

Presto, A.A., Granite, E.J., 2006. Survey of catalysts for oxidation of mercury in flue gas. Environmental Science & Technology 40 (18), 5601-5609.

Pritchard, S., 2009. Predictable SCR Co-Benefits for Mercury Control. Power Engineering 113 (1).

Pudasainee, D., Lee, S.J., Lee, S.H., Kim, J.H., Jang, H.N., Cho, S.J., Seo, Y.C., 2010. Effect of selective catalytic reactor on oxidation and enhanced removal of mercury in coal-fired power plants. Fuel 89 (4), 804-809.

Qi, G., Yang, R.T., 2004. Characterization and FTIR studies of $MnO_x\text{-}CeO_2$ catalyst for low-temperature selective catalytic reduction of NO with $NH_3$. Journal of Physical Chemistry B 108 (40), 15738-15747.

Ramis, G., Yi, L., Busca, G., Turco, M., Kotur, E., Willey, R.J., 1995. Adsorption, activation, and oxidation of ammonia over SCR catalysts. Journal of Catalysis 157 (2), 523-535.

Reddy, B.M., Durgasri, N., Kumar, T.V., Bhargava, S.K., 2012. Abatement of gas-phase mercury-recent developments. Catalysis Reviews: Science and Engineering 54 (3), 344-398.

Richardson, C., Machalek, T., Miller, S., Dene, C., Chang, R., 2002. Effect of NOx control processes on mercury speciation in utility flue gas. Journal of Air & Waste Management Association 52, 941-947.

Senior, C.L., 2006. Oxidation of mercury across selective catalytic reduction catalysts in coal-fired power plants. Journal of the Air & Waste Management Association 56 (1), 23-31.

Shan, W., Shen, W., Li, C., 2003. Structural characteristics and redox behaviors of $Ce_{1-x}Cu_xO_y$ solid solutions. Chemistry of Materials 15 (25), 4761-4767.

Si, Z., Weng, D., Wu, X., Li, J., Li, G., 2010. Structure, acidity and activity of CuOx/WOx–$ZrO_2$ catalyst for selective catalytic reduction of NO by $NH_3$. Journal of Catalysis 271 (1), 43-51.

Si, Z., Weng, D., Wu, X., Jiang, Y., Wang, B., 2011. Synergistic effects between copper and tungsten on the structural and acidic properties of CuOx/WOx-$ZrO_2$ catalyst. Catalysis Science & Technology 1, 453-461.

Topsøe, N.Y., 1994. Mechanism of the selective catalytic reduction of nitric oxide by ammonia elucidated by in situ on-line Fourier transform infrared spectroscopy. Science 265 (5176), 1217-1219.

United Nations Environment Programme, 2014. Global Mercury Assessment 2013: Sources, Emissions, Releases and Environmental Transport. UNEP Chemicals Branch, Geneva, Switzerland.

United States Environmental Protection Agency, 2011. Air Toxics Standards for Utilities. http://www.epa.gov/airquality/ powerplanttoxics/ actions.html，(accessed on December, 2015).

Wang, S.X., Zhang, L., Li, G.H., Wu, Y., Hao, J.M., Pirrone, N., Sprovieri, F., Ancora, M.P., 2010. Mercury emission and speciation of coal-fired power plants in China. Atmospheric Chemistry and Physics 10 (3), 1183-1192.

Wang, X., Rodriguez, J.A., Hanson, J.C., Gamarra, D., Martínez-Arias, A., Fernández-García, M., 2005. Unusual physical and chemical properties of Cu in $Ce_{1-x}Cu_xO_2$ oxides. The Journal of Physical Chemistry B 109 (42), 19595-19603.

Wang, Y., Ge, C., Zhan, L., Li, C., Qiao, W., Ling, L., 2012. MnOx-$CeO_2$/activated carbon honeycomb catalyst for selective catalytic reduction of NO with $NH_3$ at low temperatures. Industrial & Engineering Chemistry Research 51 (36), 11667-11673.

Wu, S., Li, H., Li, L., Wu, C.Y., Zhang, J., Shih, K., 2015. Effects of flue-gas parameters on low temperature NO reduction over a Cu-promoted $CeO_2$–$TiO_2$ catalyst. Fuel 159, 876-882.

Xu, W., He, H., Yu, Y., 2009. Deactivation of a Ce/$TiO_2$ catalyst by $SO_2$ in the selective catalytic reduction of NO by $NH_3$. The Journal of Physical Chemistry C 113 (11), 4426-4432.

Xu, W., Wang, H., Zhou, X., Zhu, T., 2014. CuO/$TiO_2$ catalysts for gas-phase $Hg^0$ catalytic oxidation. Chemical Engineering Journal 243, 380-385.

Xu, W., Yu, Y., Zhang, C., He, H., 2008. Selective catalytic reduction of NO by $NH_3$ over a $Ce/TiO_2$ catalyst. Catalysis Communications 9 (6), 1453-1457.

Yang, S., Zhu, W., Jiang, Z., Chen, Z., Wang, J., 2006. The surface properties and the activities in catalytic wet air oxidation over $CeO_2$-$TiO_2$ catalysts. Applied Surface Science 252 (24), 8499-8505.

Yao, X., Gao, F., Yu, Q., Qi, L., Tang, C., Dong, L., Chen, Y., 2013. NO reduction by CO over CuO-$CeO_2$ catalysts: effect of preparation methods. Catalysis Science & Technology 3 (5), 1355-1366.

Yao, X., Zhang, L., Li, L., Liu, L., Cao, Y., Dong, X., Gao, F., Deng, Y., Tang, C., Chen, Z., Dong, L., Chen, Y., 2014. Investigation of the structure, acidity, and catalytic performance of $CuO/Ti_{0.95}Ce_{0.05}O_2$ catalyst for the selective catalytic reduction of NO by $NH_3$ at low temperature. Applied Catalysis B: Environmental 150, 315-329.

Yu, W., Zhu, J., Qi, L., Sun, C., Gao, F., Dong, L., Chen, Y., 2011. Surface structure and catalytic properties of $MoO_3/CeO_2$ and $CuO/MoO_3/CeO_2$. Journal of Colloid and Interface Science 364 (2), 435-442.

Zhang, D., Qian, Y., Shi, L., Mai, H., Gao, R., Zhang, J., Yu, W., Cao, W., 2012. Cu-doped $CeO_2$ spheres: Synthesis, characterization, and catalytic activity. Catalysis Communications 26, 164-168.

Zhuang, Y., Thompson, J.S., Zygarlicke, C.J., Pavlish, J.H., 2004. Development of a mercury transformation model in coal combustion flue gas. Environmental Science & Technology 38 (21), 5803-5808.

List of Tables

**Table 1**. Physical properties of catalysts

| Catalysts | Surface area | Surface atomic ratio（%） | | | Temperature of first $H_2$-reduction peak (°C) |
|---|---|---|---|---|---|
| | $m^2 \cdot g^{-1}$ | $Cu^+/Cu$ | $Ce^{3+}/Ce$ | $O_\beta/O$ | |
| CuTi | 66.8 | 65.3 | - | 10.5 | 180 |
| CeTi | 101.4 | - | 23.1 | 15.7 | 503 |
| CuCeTi | 95.0 | 72.0 | 29.7 | 21.4 | 160 |

$O_\beta$: chemically adsorbed oxygen/weakly bonded oxygen.

List of Figures

**Figure 1.** Schematic diagram of the experimental setup

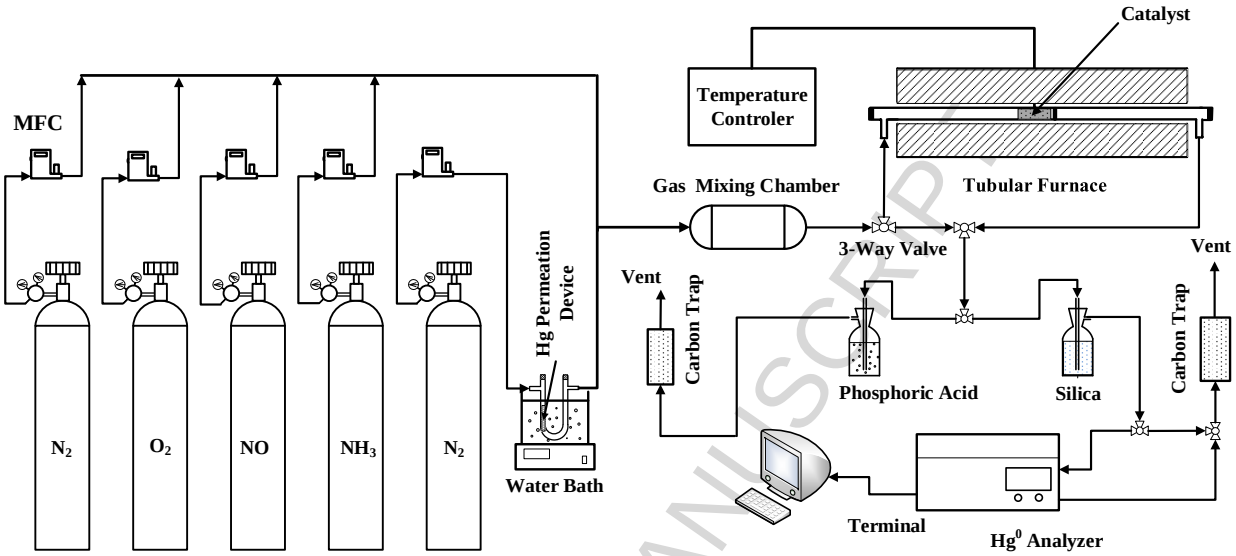

**Figure 2.** (a) Cu 2p XPS patterns of CuTi, and CuCeTi catalysts; (b) Ce 3d patterns of CeTi and CuCeTi catalysts

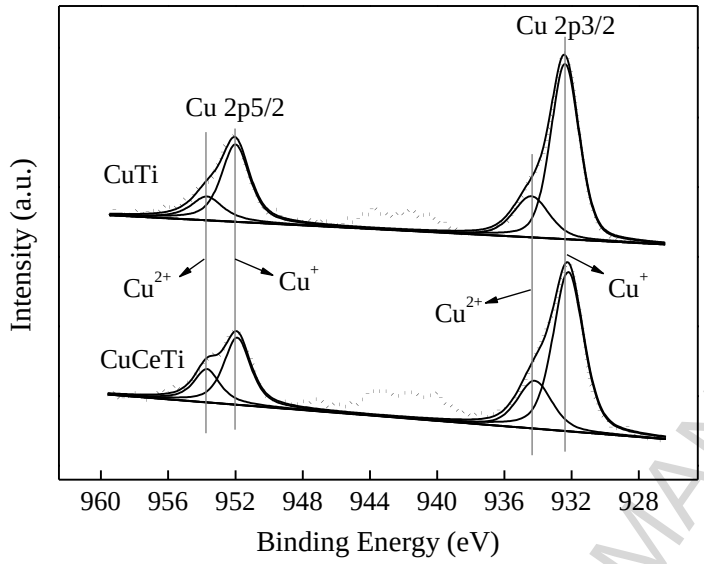


(a)

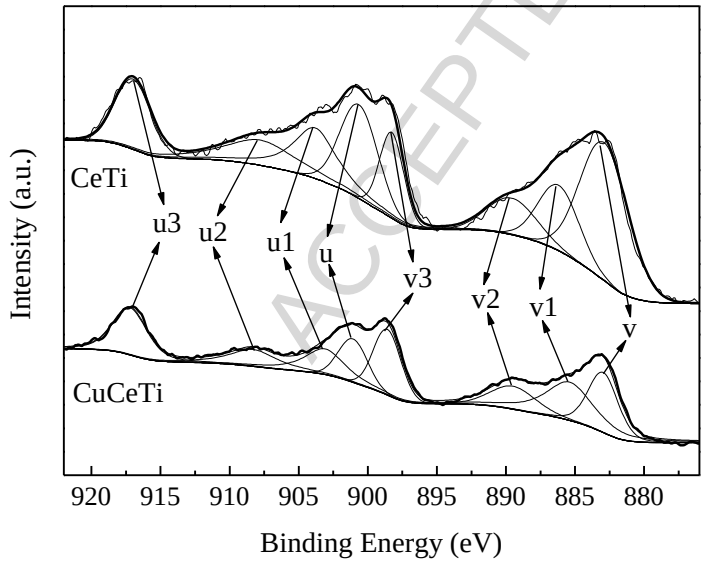


(b)

**Figure 3.** $Hg^0$ oxidation over CuTi, CeTi and CuCeTi catalysts under SCR atmosphere at 200 °C

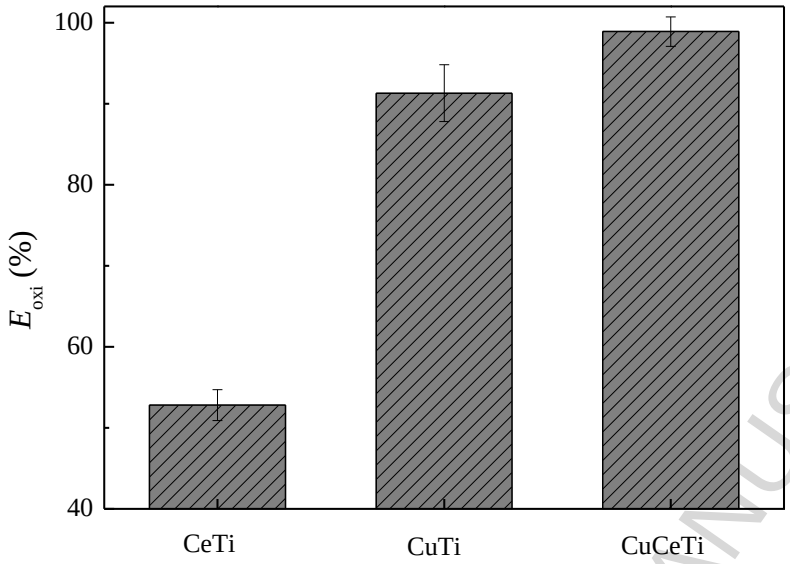

**Figure 4.** $Hg^0$ oxidation over CuTi, CeTi and CuCeTi catalysts in the presence of NO

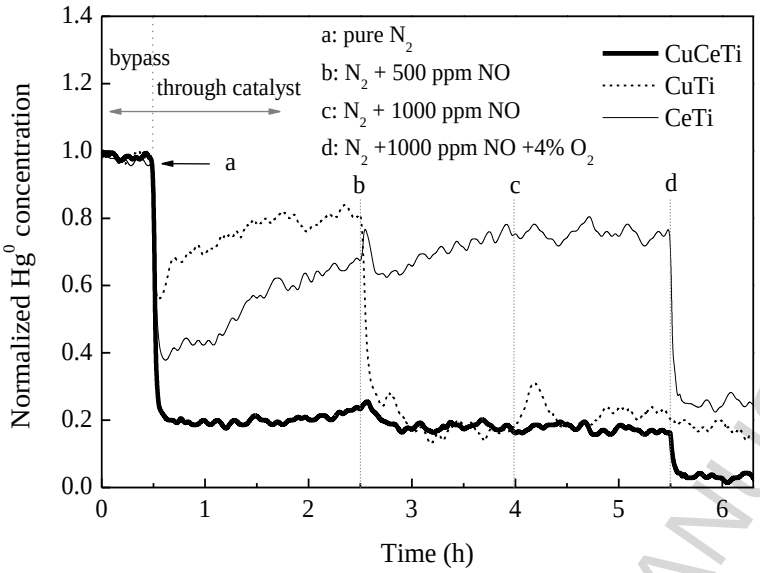

**Figure 5.** $Hg^0$ physical adsorption over CuCeTi catalyst at room temperature

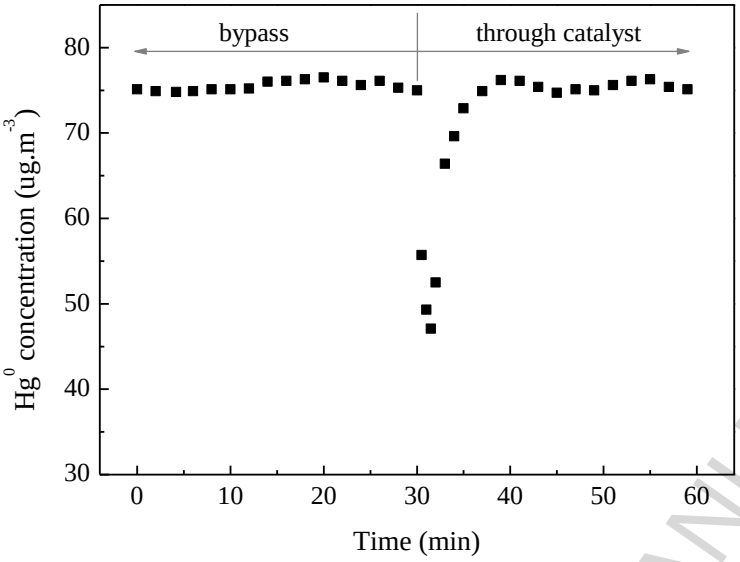

**Figure 6.** $Hg^0$ oxidation over CuTi, CeTi and CuCeTi catalysts in the presence of $NH_3$

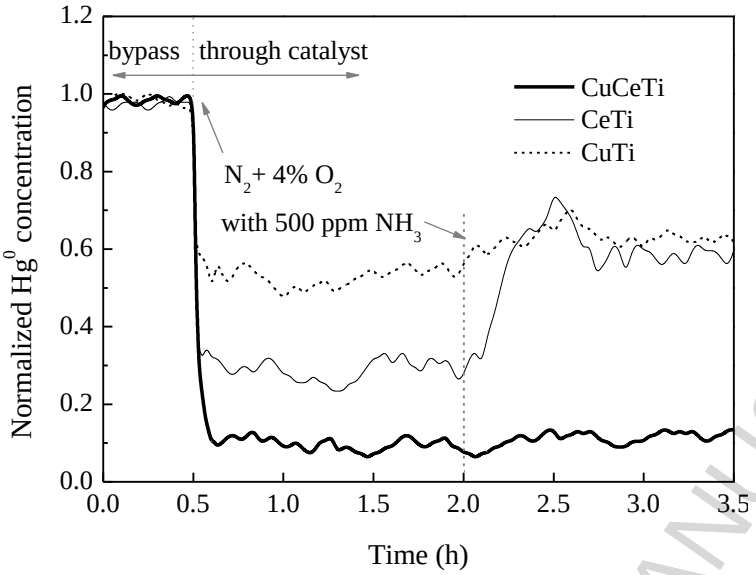

**Figure 7.** Effect of $NH_3$ on $Hg^0$ oxidation over CuCeTi catalyst in the presence of $O_2$ and NO

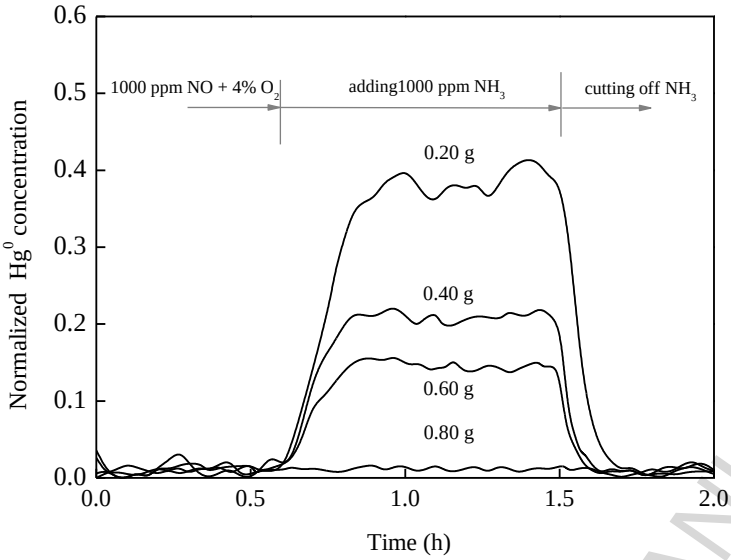

**Highlights**

> Combination of CuO and $CeO_2$ yielded synergy for $Hg^0$ oxidation under SCR atmosphere. > 99.0% $Hg^0$ oxidation rate was observed on the CuCeTi catalyst at 200 °C and high GHSV. > Enough Lewis acid sites scavenged the competitive adsorption between $NH_3$ and $Hg^0$. > Complete recovery of $Hg^0$ oxidation activity was quickly achieved after cutting off $NH_3$.